Biochimica et Biophysica Acta 1840 (2014) 745–756

Contents lists available at ScienceDirect

Biochimica et Biophysica Acta

journal homepage: www.elsevier.com/locate/bbagen

Review

Genetically encoded fluorescent redox sensors ☆

Konstantin A. Lukyanov, Vsevolod V. Belousov *

Shemyakin-Ovchinnikov Institute of Bioorganic Chemistry, Miklukho-Maklaya 16/10, Moscow 117997, Russia

ARTICLE INFO

Article history:
Received 24 February 2013
Received in revised form 10 May 2013
Accepted 20 May 2013
Available online 29 May 2013

Keywords:
Fluorescent protein
HyPer
rxYFP
roGFP

ABSTRACT

Background: Life is a constant flow of electrons via redox couples. Redox reactions determine many if not all major cellular functions. Until recently, redox processes remained hidden from direct observation in living systems due to the lack of adequate methodology. Over the last years, imaging tools including small molecule probes and genetically encoded sensors appeared, which provided, for the first time, an opportunity to visualize and, in some cases, quantify redox reactions in live cells. Genetically encoded fluorescent redox probes, such as HyPer, rxYFP and roGFPs, have been used in several models, ranging from cultured cells to transgenic animals, and now enough information has been collected to highlight advantages and pitfalls of these probes.
Scope of review: In this review, we describe the main types of genetically encoded redox probes, their essential properties, advantages and disadvantages. We also provide an overview of the most important, in our opinion, results obtained using these probes. Finally, we discuss redox-dependent photoconversions of GFP and other prospective directions in redox probe development.
Major conclusions: Fluorescent protein-based redox probes have important advantages such as high specificity, possibility of transgenesis and fine subcellular targeting. For proper selection of a redox sensor for a particular model, it is important to understand that HyPer and roGFP2-Orp1 are the probes for H_2O_2, whereas roGFP1/2, rxYFP and roGFP2-Grx1 are the probes for GSH/GSSG redox state. Possible pH changes should be carefully controlled in experiments with HyPer and rxYFP.
General significance: Genetically encoded redox probes are the only instruments allowing real-time monitoring of reactive oxygen species and thiol redox state in living cells and tissues. We believe that in the near future the palette of FP-based redox probes will be expanded to red and far-red parts of the spectrum and to other important reactive species such as NO, O_2 and superoxide. This article is part of a Special Issue entitled Current methods to study reactive oxygen species - pros and cons and biophysics of membrane proteins. Guest Editor: Christine Winterbourn.

1. Introduction

Green fluorescent protein (GFP) from the jellyfish *Aequorea victoria* and homologous fluorescent proteins (FPs) of different colors from diverse marine creatures fluoresce due to their unique chromophore groups. Chromophores appear inside the proteins by cyclization and oxidation (by molecular oxygen) of the protein backbone at specific positions; this process requires no external cofactors or enzymatic activities [1,2]. Due to their unique ability for self-catalyzed chromophore formation, FPs are widely used as fluorescent probes that are fully genetically encoded in a single gene [3]. An FP-encoding gene can be introduced to a model organism resulting in expression of the functional fluorescent protein, which can be detected by fluorescence microscopy, flow cytometry and other fluorescence-based methods.

FPs revolutionized biomedical research [4]. When Osamu Shimomura and colleagues were extracting green fluorescent protein from *A. victoria* in the early 1960s [5], they would not have imagined how many applications GFP would find in biology. There are several main areas of FP applications [3]. First, activity of target gene promoters can be monitored by placing FP under their control. Using this tool, one can reveal spatial and temporal patterns of gene activities, follow the fates of specific cell populations, or to visualize cells of intricate shapes (such as neurons). Second, FP encoded in frame with a target protein enables visualization of the intracellular distribution and dynamics of proteins of interest. Third, protein–protein interactions can be monitored by fluorescence (Forster) resonance energy transfer (FRET) between FPs of appropriate colors (e.g., cyan and yellow, or green and red) [6]. Finally, perhaps the most sophisticated field is construction of genetically encoded fluorescent indicators (GEFIs) for ions, small molecules, and enzymatic activities [3,7]. Sensors enable real-time monitoring of secondary messengers, activation of signaling cascades, cell–cell communication, neuron activity, etc. Currently, more than a hundred different GEFIs exist. Some of them are widely used, some of them not, but their overall number highlights the virtually unlimited variety of functional

☆ This article is part of a Special Issue entitled Current methods to study reactive oxygen species - pros and cons and biophysics of membrane proteins. Guest Editor: Christine Winterbourn.

* Corresponding author. Tel.: +7 499 7248122; fax: +7 495 3307056.
E-mail address: vsevolod.belousov@gmail.com (V.V. Belousov).

0304-4165/$ – see front matter © 2013 Elsevier B.V. All rights reserved.
http://dx.doi.org/10.1016/j.bbagen.2013.05.030

combinations of FPs and other protein domains, which result in environment-sensitive fluorescence.

Except in rare cases when FP itself is sensitive to environmental factors (such as pH), a sensor should include some sensitive protein domains, which will determine a specific response to a particular analyte or activity [3]. Fluorescence readout of sensors can differ. Most available sensors are based on change of FRET efficiency between two FPs resulting from conformational changes of sensitive domains [8]. Another popular design of sensors is based on circularly permuted (cp) FPs, in which original N- and C-ends are connected and new N- and C-ends are created [9,10]. cpFPs with termini spatially close to the chromophore are potentially highly responsive to conformational changes of sensitive domains fused to them. Regardless of design, creation of a new sensor usually represents a laborious and time-consuming activity. Selection of appropriately sensitive domains and FPs, as well as further careful optimization of relative positions of all protein domains and linkers between them is required to create a sensor with high selectivity and specificity and a clear fluorescence response.

The present review is focused on genetically encoded redox probes, their advantages and limitations. Several years have passed since the first introduction of such probes to researchers, enough time to prove that the technology works and to collect initial sets of data. We shall give an overview of the most important results obtained using redox GEFIs.

2. Genetically encoded indicators: general principles

2.1. Simple single FP-based sensors

There are several types of GEFI design. A detailed description of all of them is beyond the scope of the current review. Instead, we briefly describe the most widely used principles for sensors (Fig. 1). In the simplest GEFIs the intrinsic FP chromophore sensitivity to small ions is used to trace changes in concentration of the ions. The most common examples of such GEFIs are the sensors for pH [11,12] and chloride [13–17]. The chromophore of the wild type GFP from *A. victoria* (avGFP) is sensitive to pH, and most of the yellow fluorescent variants of avGFP are sensitive to Cl^-. The strategy for improvement of such sensors is site-directed and involves random mutagenesis in search for mutants with enhanced H^+ or Cl^- sensitivity and large dynamic range ($\Delta F/F_0$). Since the chromophore of FP is deeply buried inside the β-barrel structure and not accessible to large molecules, the number of substances that can be measured using single FP sensors with non-modified β-barrel is limited to a few small ions.

2.2. FRET-based sensors

The second type of GEFI has the largest number of published variants. These sensors are based on FRET between two FPs [6,8,18–20]. The basic fact underlying FRET is energy transfer from a light-excited fluorophore (donor fluorophore) to a longer wavelength chromophore (acceptor) whose absorption spectrum overlaps with the emission spectrum of the donor. FRET works at short distances between the chromophores (better less than 5 nm) and requires optimal angles between the chromophore planes. Therefore, good FRET is not easy to achieve. Induction of FRET leads to several changes in spectral properties of the system. First, fluorescence intensity of the donor fluorophore drops since some of the energy starts to be absorbed by the acceptor fluorophore. Second, the fluorescence intensity of the acceptor increases (if the acceptor is fluorescent) due to the appearance of additional source of excitation. Third, the fluorescence-excited-state lifetime of the donor decreases because additional energy is dissipated by channeling to the acceptor. Based on these facts, several readouts can be used to evaluate FRET changes: ratio between donor and acceptor fluorescence, the increase in donor fluorescence upon acceptor photobleaching, and measurement of the donor fluorescence lifetime [8].

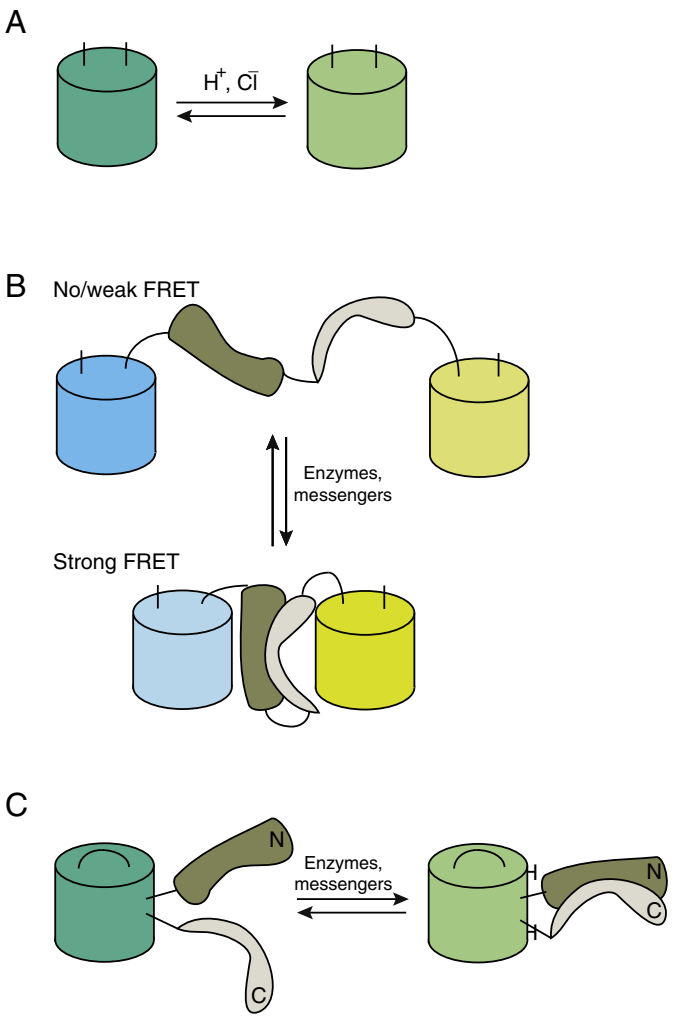

Fig. 1. Major types of GEFIs. A. The simplest GEFIs are based on intrinsic sensitivity of some of the FPs to small ions such as H^+ or Cl^-. Changes in concentration of the ions are reflected in spectral shifts. B. FRET-based sensors explore conformation changes in a linker flanked by two FPs comprising a FRET pair. Structural rearrangements of the domains comprising the linker lead to changes in FRET efficiency. C. Sensors based on circularly permuted proteins consist of cpFP fused to domain(s) undergoing conformation changes upon interaction with an environment.

The idea behind the genetically encoded FRET-based sensors is to fuse two FPs comprising a FRET pair into a single polypeptide chain with sensing protein domain(s) able to change the conformation upon interaction with a substance of interest and therefore change the distance/angle between the donor and the acceptor, thereby changing FRET. There are a number of designs for such sensors, from simple proteolytic cleavage site between FPs to large complex linkers in GEFIs for kinases consisting of a kinase docking site, a phosphorylation site and a phospho-amino acid recognition motif flanked by the donor and the acceptor FPs [8,21].

The main advantage of the FRET-based probes is a ratiometric signal, enabling the ratio between two wavelengths to be measured. In contrast to a single-wavelength readout, a ratiometric signal does not depend on the concentration of the sensor in the cell or in a cellular compartment, and thus artifacts arising from cell movement, changes of shape or cytoplasm condensation can be avoided. The main disadvantages of the FRET GEFIs are low dynamic range, large molecular weight complicating subcellular targeting, and occupation of a broad part of the spectrum. Most of the FPs are more or less sensitive to pH and, therefore, FRET sensors with two different chromophores may have complex pH-driven responses.

2.3. Sensors based on circularly permuted FPs

Perhaps the most promising type of GEFI is based on a single FP modified using circular permutation. The β-barrel of the GFP is very rigid and therefore unlikely to change conformation in response to forces applied to its termini. In a procedure named circular permutation the original N- and C-termini are fused by a short (6–10 a.a.) polypeptide linker and new termini are introduced at the side of the β-barrel near the chromophore [9,10]. Circularly permuted FPs (cpFPs) are sensitive to conformational distortions induced by movements of the environment-sensing domains fused to their termini. Changes in structure or interactions of the sensing domains cause changes in the FP chromophore environment and spectral properties of the sensor.

The first cpFP sensors utilized protein–protein interactions between the two domains fused to N- and C-termini of the cpFP in response to changes in Ca^{2+} [22,23]. In HyPer, a GEFI for H_2O_2 [24], we developed a simple design of sensor construction using a minimal set of domains: one cpFP and one sensing domain (see below). To date a number of sensors have been constructed using this "minimalistic" design. Examples are the GEFIs for ATP/ADP [25], NAD^+/NADH [26], organic hydro peroxides [27] and others. The major drawback of the first generation of cpFP-based GEFIs is their high pH sensitivity. This issue can be addressed by using appropriate controls, and the user can take advantage of their smaller size and much higher dynamic range compared to FRET-based probes. The release of cpFP-based GEFIs for Ca^{2+} promises more pH-stable and spectrally diversified probes [28].

2.4. Translocation-based sensors

Another important class of GEFIs reports intracellular events by translocation readout [29]. The design of the translocation-based GEFIs is usually based on fusing FP with protein domains that change position in the cell under particular parameter changes. The major type of translocating sensor is used to image specific phosphoinositides in cellular membranes [30–32]. An inositol ring of phosphatidylinositol (PI) is subject to phosphorylation and dephosphorylation at various positions on the ring. Each particular form of phosphorylated PI is a messenger recognized by specific domains. Fusing GFP with one such domain enables dynamic imaging of the messenger by following translocation of the fluorescence to/from the plasma membrane. Other examples of translocating GEFIs include those redistributing between the cytoplasm and the nucleus [33,34].

2.5. Other sensors

There are several other types of GEFIs that utilize the photoconversion ability of some FPs [35], split-GFP [36,37] technology and introduction of specific amino acids to the GFP barrel [38–40]. The latest type of sensors is important in the context of this review since they include a class of engineered redox-sensitive FPs (see below).

3. Genetically encoded redox probes

Since the discovery of ROS there have been numerous attempts to develop tools to measure these short-living molecules in a physiological context. While many fluorogenic, colorimetric and luminescent probes enabled the measurement of some ROS with a high degree of accuracy, intracellular ROS imaging methods have performed poorly and have suffered from many artifacts [41–44]. The situation with regard to measuring the redox state of thiols in living cells was even worse: there were no methods to image the intracellular GSH/GSSG ratio. GEFIs appear to be ideal tools to fill this methodological gap.

Normally, a living cell, alone, or as part of a multicellular organism, receives information about each particular parameter inside and outside of the cell. Living organisms evolved highly specialized sensing proteins that transduce changes in the parameter measured to transcriptional or enzymatic responses. Redox-related processes are not an exception. For example, an *Escherichia coli* cell is able to separately measure a superoxide anion radical by means of a 2Fe-2S cluster protein SoxR [45] and hydrogen peroxide by redox active cysteines of OxyR [46]. Although H_2O_2 is almost entirely a product of superoxide dismutation, the cell "prefers" to measure them separately. This gives us a unique opportunity to use these domains in GEFIs.

3.1. Hydrogen peroxide sensor HyPer

When designing HyPer (Fig. 2) we utilized the ability of the *E. coli* transcription regulator OxyR to selectively sense tiny amounts of H_2O_2 by its regulatory domain, OxyR-RD [46]. OxyR-RD contains several Cys residues, two of which are critical for H_2O_2 sensing. Cys199 has two features important for protein function: it has low pKa due to an adjacent Arg residue and is positioned in a hydrophobic surrounding [47]. Low pKa makes Cys199 able to react with H_2O_2 with a rate constant of 10^5–10^7 M^{-1} s^{-1} [48,49]. A hydrophobic pocket restricts penetration of charged oxidants such as the superoxide anion radical, in contrast to amphiphilic H_2O_2. Being oxidized to charged sulfenic acid and repelled by the hydrophobic pocket, Cys199 gets close to Cys208 and they form disulfide bond [47]. Disulfide formation results in profound conformational changes in the OxyR-RD fold. Integration of cpYFP into the conformation-changing region in OxyR-RD, between residues 205 and 206, resulted in HyPer, a GEFI for H_2O_2 detection [24]. HyPer has

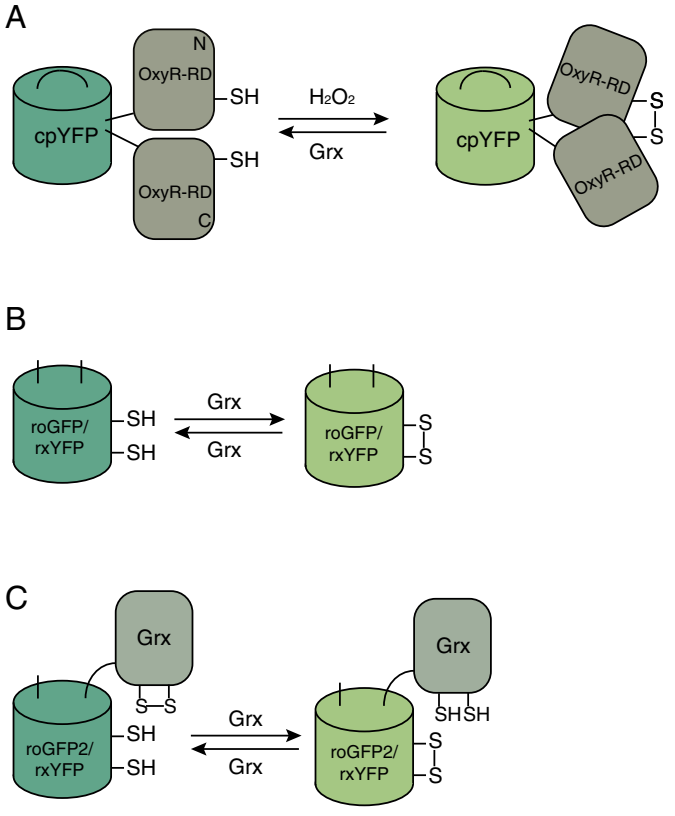

Fig. 2. Popular redox GEFIs. A. HyPer consists of cpYFP integrated into the OxyR-RD H_2O_2 sensing domain in a way that allows intramolecular disulfide formation in OxyR-RD to be reflected in cpYFP ratiometric excitation spectrum changes. B. rxYFP and roGFPs contain pairs of Cys residues capable of intramolecular disulfide formation upon equilibration with the cellular thiol pool. Inside the cell, this equilibration is catalyzed by glutaredoxins and proceeds slowly. C. Fusing rxYFP and roGFP2 with Grx resulted in very fast equilibration of the redox GEFIs with the cellular thiol pool. Changing Grx for Orp1 peroxidase in the fusion with roGFP2 converts the sensor into the H_2O_2 probe.

two excitation peaks with maxima at 420 nm and 500 nm and one emission peak at 516 nm. Oxidation of HyPer by H_2O_2 results in a decrease in the 420-nm excitation peak and a proportional increase in the 500-nm excitation peak, making the sensor ratiometric. As mentioned above, ratiometric readout prevents many imaging artifacts caused by object movement and different expression levels between cells or compartments. The great advantage of HyPer is its reversibility: similar to oxidized OxyR it can be reduced by cellular thiol-reducing systems. High sensitivity to H_2O_2 (low-to-middle nanomolar range) [24], fast reaction rate constant (10^5 M^{-1} s^{-1}) [50] and reversibility [24] makes HyPer an invaluable tool to monitor real-time dynamics of H_2O_2 in the living cell.

OxyR and therefore HyPer have midpoint potential of the redox-active Cys pair of −185 mV [46]. Thus, HyPer can be used only in the relatively reducing environment of the nucleocytoplasmic compartment [24,51,52], mitochondria [24,51] and peroxisomes [51,53,54], but not outside the cell or in the lumen of endosomes and the endoplasmic reticulum. Although one study reported reduced HyPer in the ER lumen [55], several attempts to express ER-targeted HyPer resulted in a completely oxidized sensor [51,56].

The bacterial nature of OxyR-RD has one more advantage: it has virtually no interaction partners within mammalian cells. Therefore, it is less toxic upon overexpression, and less subjected to post-translational modifications that may result in false-negative or false-positive signals.

Important features of GEFIs, including HyPer, result from their proteinaceous nature. By adding a simple subcellular localization tag to the protein sequence it is possible to target it to a specific compartment of the cell, be it the nucleus, mitochondrial intermembrane space, or peroxisome [51]. Moreover, it can be fused with various proteins of interest, just like regular GFP, therefore ensuring sub-compartmental measuring of H_2O_2 [52].

Recently, two enhanced versions of HyPer have been developed, namely HyPer-2 [57] and HyPer-3 [50]. HyPer-2 is a product of occasional point mutation in the dimeric interface of the OxyR-RD domain of the probe. HyPer-2 has an expanded dynamic range (6–7 compared to 3 in HyPer) and higher brightness upon expression in eukaryotic cells (Belousov et. al, unpublished observation). However, HyPer-2 has two times slower oxidation and reduction rates in vitro. With HyPer-3, the problem of slow response has been solved: thus, both oxidation and reduction rates have been improved considerably compared to HyPer-2 while keeping its dynamic range high.

The chromophore of wtGFP and almost all GFP-like proteins contains a Tyr residue that can be either protonated (neutral) or deprotonated (anionic) [58–60]. In pH-sensitive proteins the chromophore environment is organized in a way that allows proton transfer from chromophore Tyr to the media [59]. Therefore, changes in pH lead to changes in chromophore protonation. Having a broken barrel structure, most cpFPs have a chromophore connected to the outer space meaning they are pH-sensitive. HyPer is no exception here having strong pH sensitivity. Its 420 nm and 500 nm excitation peaks correspond to protonated and anionic forms of the chromophore, respectively. Acidification of the environment leads to an increase in the protonated form (ex. 420 nm) and a decrease in the deprotonated form (ex. 500 nm), therefore mimicking reduction of the probe [24,61]. Alkalization, in contrast, mimics oxidation of HyPer. The pH problem can be solved by using pH-specific probes as a control. An ideal control for HyPer is its H_2O_2-insensitive version HyPer-C199S. This mutant was originally used to show that Cys199 in HyPer plays the same role as in OxyR [24]. Later, HyPer-C199S was "rediscovered" under the name of SypHer [61]. The pH dependency of SypHer has been characterized in detail and the indicator was successfully used to track pH changes in the cytoplasm and in the mitochondria [61]. Since SypHer has exactly the same pH sensitivity as HyPer, it can serve as the most relevant pH control. Other options to monitor pH include a number of pH-responsive FPs [62,63] and small molecule dyes, some of which have distinct spectra allowing pH detection in the same cells using multiparameter imaging.

3.2. Redox GFPs and their modifications

3.2.1. rxYFP

The redox state of cysteines in proteins equilibrates with the GSH/GSSG ratio by thiol-disulfide exchanging enzymes such as glutaredoxins. Therefore introducing cysteines near the FP chromophore could result in proteins that change their spectra upon oxidation/reduction. The first attempt to make such a protein by Ostergaard and colleagues in the laboratory of Jacob Winther resulted in redox-active YFP (rxYFP) having mutations N149C and S202C [38]. These amino acids are surface residues positioned in the neighboring β-strands and both are close to the chromophore. The positions 148 and 203, adjacent to the mutated 149 and 202, face the chromophore and form the microenvironment critical for its fluorescence. Formation of C149–C202 disulfide in rxYFP leads to changes in the H148 and Y203 positions relative to the chromophore and results in spectral changes. The absorption spectrum changes in a ratiometric way upon oxidation: the 404 nm peak decreases while the 512 nm peak increases within a dynamic range of the ratio Abs512/Abs404 of about 4. However, the 404 nm peak is non-fluorescent and therefore only the 512 nm peak can be used for imaging. This makes the probe intensiometric with a dynamic range of ~2. The detailed protocol of rxYFP imaging can be used to set up imaging parameters and to quantify the results [64]. Unfortunately, no variants of rxYFP with ratiometric readout have been published. Potentially, this work could be done by Y203F substitution, which is known to make the protonated form of YFP chromophore fluorescent [22,24].

The midpoint potential of rxYFP is −261 mV. When purified, the protein equilibrates very slowly with glutathione in different redox states. However, addition of recombinant glutaredoxin significantly accelerates the reaction [65]. It has become clear that glutaredoxin availability is a bottle neck in rxYFP technology. In their paper, Björnberg and co-authors wrote: "We were interested in characterizing the interaction between yeast Grx1p and its synthetic substrate rxYFP and obtaining a redox sensor independent of the availability of Grx in the experimental host organism. We therefore constructed a fusion of the two proteins, rxYFP-Grx1p, which efficiently equilibrates the sensor with a glutathione redox buffer and provides new insight into the mechanism of Grx" [66]. Later, this clever idea led Tobias Dick to make another redox active protein, roGFP2, in its form fused to glutaredoxin, a useful tool to study thiol redox potential in vivo [67].

3.2.2. roGFPs

The idea of introducing cysteines directly into the GFP, first used to make rxYFP, was later applied to wild type avGFP [39,40]. Introducing Cys residues in place of S147 and Q204, again close to positions 148 and 203 facing the chromophore, and mutation C48S, resulted in roGFP1. The introduction of the S65T mutation to roGFP1 resulted in roGFP2 [39,40]. Both sensors have two excitation peaks corresponding to the protonated and anionic forms of the chromophore. Oxidation of both roGFPs results in changes in the chromophore protonation state, increasing the protonated form excitation band (400 nm) and decreasing the anionic form excitation band (475 nm for roGFP1 and 490 nm for roGFP2) [39,40]. So, in contrast to rxYFP, roGFPs provide ratiometric fluorescence readout. Both roGFPs have lower midpoint potential (−291 mV for roGFP1 and −280 mV for roGFP2) compared to rxYFP (−261 mV) making them more sensitive to small changes in the GSH/GSSG oxidation state of the reducing environment. The relationship between redox potential and oxidation state, as well as many other aspects of roGFPs and rxYFP are discussed in detail in the review by Meyer and Dick [68].

In practical terms, roGFP2 appears to be more useful than roGFP1 for several reasons. First, roGFP2 is brighter and has a higher dynamic range when excited with conventional laser wavelengths, 405 nm and 488 nm. Second, in roGFP2 the anionic form of the chromophore (ex. 490 nm) dominates over the protonated form (ex. 400 nm), while the opposite is true for roGFP1 [39]. Since the anionic form decreases upon oxidation and the protonated form increases, oxidation

of roGFP1 results in a decrease in the weak signal (anionic) and an increase in an initially strong signal (protonated). With roGFP2, the strong anionic form decreases and the weak protonated form increases making imaging easier.

While roGFP1 is pH-insensitive, roGFP2 is sensitive to pH with pKa of ~6 [39]. However, the original publication [39] reports only the pKa value without providing details on spectra changes. Later, Gutscher et al. reported that both protonated and anionic forms of the roGFP2 chromophore decrease upon acidification without affecting the ratio between them [67]. Therefore the ratiometric readout is pH-stable. However, pH shifts the thiol-disulfide equilibrium thereby affecting the roGFP2 response [39]. Nevertheless, the roGFP2 ratiometric readout can be considered to be more-or-less pH-insensitive since the pKa for most of the cysteines in the cell, including those in roGFPs, is close to 9, far greater than physiological pH values.

3.2.3. Grx1-roGFP2

The problem of the slow equilibration with external thiols described for rxYFP persists in roGFPs [69]. The reaction of thiol-disulfide exchange between glutathione and roGFPs is catalyzed by glutaredoxin. Availability of glutaredoxin is therefore a rate-limiting factor in roGFPs equilibration with intracellular thiols. As mentioned above, this issue had been solved for rxYFP by equipping each rxYFP molecule with Grx via fusing the two proteins [66]. Gutscher and colleagues successfully applied this scheme to roGFP2 and significantly improved performance of the probe [67]. In vitro, Grx1-RoGFP2 responded to either GSH or GSSG in a time scale of minutes, whereas roGFP2 alone was not reactive at all under the same conditions. Moreover, Grx1-RoGFP2 was sensitive to even small traces of GSSG in commercial samples of GSH. Grx1-RoGFP2 senses redox potential changes between −240 mV and −320 mV. This range corresponds to very minor concentrations of GSSG (midpoint potential of glutathione is ~−180 mV). Whereas the probe was insensitive to H_2O_2, addition of GSH led to H_2O_2-induced oxidation of the sensor, indicating that H_2O_2 influences the sensor only via oxidation of GSH. This is very important since roGFPs are often incorrectly interpreted and used as probes for ROS. The belief in roGFPs as ROS sensors stems from the common misconception that all cysteines are highly redox reactive, whereas this is true only for the minor portion of Cys residues with low pKa that are deprotonated at physiological pH. This is not the case for cysteines in roGFPs, which are regular cysteines that react only with millimolar amounts of oxidants. However, enzymatic oxidation of such cysteines is still possible, as Grx1-RoGFP2 illustrates. Grx1-RoGFP2 is currently the probe of choice for measuring the 2GSH/GSSG ratio in highly reduced compartments. Morgan and colleagues provide detailed protocols for using roGFP2-based probes [70].

3.2.4. Orp1-roGFP2

Successful development of Grx1-roGFP2 led Tobias Dick and colleagues to propose using roGFP2 as a substrate for a peroxidase [71]. Thus, if the peroxidase uses H_2O_2 as one substrate, it could use roGFP2 as its reducing substrate, if both proteins were fused together. Indeed, fusing roGFP2 with yeast peroxidase Orp1 resulted in a H_2O_2 probe with the spectral properties of roGFP2: ratiometric pH-stable readout reporting submicromolar H_2O_2 [71]. The primary aim of the investigation was to understand better a mechanism of thiol oxidation in vivo. It was known that most of the cysteines are not very reactive with H_2O_2. Even those that are redox-reactive, like catalytic Cys in PTP-1B tyrosine phosphatase [72,73], react with H_2O_2 rather slowly compared to abundant peroxiredoxins [74]. It is not clear, therefore, how such cysteines get oxidized in the presence of multiple Prx enzymes. One explanation could be that those cysteines do not react directly with H_2O_2 but rather undergo oxidation mediated by peroxidases. Being a part of a redox relay where Orp1, being oxidized by H_2O_2, oxidizes transcription factor Yap1, Orp1 was a good model of such peroxidase [75], and roGFP2 with its surface cysteines was a good potential partner for such peroxidase. Indeed, it was demonstrated that, being fused with roGFP2, Orp1 catalyzes near stoichiometric conversion of H_2O_2 to disulfides in roGFP2. Two most important conclusions from these experiments are: i) that some peroxidases catalyze oxidation of proximal cysteines even if the cysteines are not highly redox-active and ii) the utility of Orp1-roGFP2 as a probe for H_2O_2. A direct comparison of Orp1-roGFP2 with HyPer revealed similar profiles of response to H_2O_2 in the cytoplasm of mammalian cells. HyPer demonstrated faster oxidation in agreement with the different mechanisms of probe oxidation: direct reaction of HyPer and peroxidase-mediated reaction of Orp1-roGFP2 [71].

3.3. FRET-based sensors

Several attempts have been made to make a FRET-based probe for H_2O_2. The first examples consisted of an ECFP-EYFP FRET pair connected by a linker having two Cys residues able to form disulfide upon oxidation [76]. In fact, the properties of this Cys pair should not differ too much from those in roGFP: slow equilibration with thiols in the absence of a personal Grx. However, the dynamic ranges of the probes were too small to be useful for imaging. Optimization of the linker composition and the FRET pair resulted in a sensor with a 6 fold change in FRET efficiency and a midpoint potential of −143 mV [77]. The probe was suggested to be suitable for redox imaging in oxidized compartments, such as ER. Later the probe was used to measure E_{GSH} in the ER lumen [78]. The midpoint potential of the probe is more than 80 mV less negative than that of roGFP1-iX [79] (−229 mV), a specially designed roGFP1 version with improved performance under oxidizing conditions.

Recently, two novel FRET probes were developed by Enyedi and colleagues [80]. One of the sensors, OxyFRET, contains two cysteine-reach domains (CRD) of Yap1 (a component of the Orp1–Yap1 redox relay) separating cyan and yellow FPs. Oxidation in the CRDs results in FRET change, however the cellular machinery responsible for oxidation remains to be identified. The second probe, PerFRET consists of one CRD domain and Orp1 peroxidase flanked by the FRET pair. Here an active mechanism for oxidation has been suggested. Nevertheless, both sensors have similar performance in different cell culture models. Although the dynamic range of the probes is rather small, they were successfully used to monitor NADPH oxidase activation. Importantly, the probes performed correctly in fusions with other domains [80].

3.4. A case of cpYFP: superoxide vs. pH sensing

Recently, a circularly permuted YFP was reported to sense the superoxide anion radical, $O_2^{\bullet-}$, in the mitochondrial matrix [81]. By expressing mito-cpYFP in cardiac myocytes, the authors were able to detect "flashes" of superoxide. In isolation, the probe demonstrated an increase in fluorescence upon incubation with xanthine/xanthine oxidase in a SOD-sensitive manner. SOD mimetics and antioxidants decreased the frequency of the "flashes". This controversial paper [81] attracted substantial criticism and discussion. Initial criticism was focused on the fact that flashes are preserved under anoxic or hypoxic conditions where the $O_2^{\bullet-}$ cannot be formed due to a lack of oxygen [82]. Effects of pharmacological inhibitors of ETC on the superoxide flashes also raised criticism [82]. For example, Antimycin A, an inhibitor of Complex III known to induce superoxide production by the ETC, inhibited the flashes [81].

Several more recent pieces of evidence suggested that cpYFP is not a superoxide but pH sensor. Thus, Schwarzlander and colleagues evaluated cpYFP in plant mitochondria and found similar flashes, but were unable to modify their intensity or frequency by manipulating mitochondrial $O_2^{\bullet-}$ [83]. Nevertheless, cpYFP responded to manipulations with matrix pH. Describing cpYFP flashes, Wang et al. used EYFP as a control for pH changes, despite EYFP differing substantially from cpYFP in pH sensitivity: at pH values characteristic for mitochondrial matrix (7.5–8.5) EYFP demonstrated 10 fold less change in fluorescence and could not be used as a control [84].

Does cpYFP sense superoxide or pH? Mito-HyPer and mito-SypHer, which are also cpYFP-based probes, were able to detect similar mitochondrial flashes [85]. Interestingly, the flashes occurred simultaneously with an increase in red fluorescence from another superoxide sensor, MitoSox, which is pH-stable in the physiological range of pH [85]. However, even if we believe that MitoSOX is a relevant probe for superoxide, the rise in $O_2^{\bullet-}$ could be a consequence of pH increase, as the rate of superoxide dismutation depends on pH. The spontaneous dismutation rate falls by a factor of 10 with each unit increase in pH. The SOD-catalyzed process is less pH-dependent. Therefore, it may turn out that both processes, pH increase and $O_2^{\bullet-}$ formation/stabilization take place.

Given that the mechanism of cpYFP sensitivity to superoxide has not been described and the existence of superoxide flashes not cross-validated with different methods, it is clear that more experiments are necessary to prove the utility of cpYFP as a probe for $O_2^{\bullet-}$. Experiments with the pH-insensitive probe mito-Orp1-roGFP2 [71] would be helpful as H_2O_2 provides a relatively good readout for superoxide production.

3.5. NAD^+/NADH GEFIs

NAD^+/NADH and $NADP^+$/NADPH are two redox pairs that provide reducing equivalents to all downstream redox systems. Whereas NAD^+/NADH couple is mainly used in fuel oxidation reactions, $NADP^+$/NADPH provides electrons for anabolic processes [86]. Both redox couples are involved in ROS production/decomposition. In mitochondria, electrons from NADH can leak from the electron transport chain to oxygen and produce superoxide [87]. In cytoplasm, electrons from NADPH are used by NADPH oxidases to produce superoxide [88] and, at the same time, to support antioxidant systems [89]. Whereas NADP exists in the cell mostly in its reduced form, NAD is predominantly oxidized. Recently, two GEFIs for NAD^+/NADH named Peredox and Frex were developed [26,90]. Both of them are based on integration of a circularly permuted FP into bacterial Rex family domains. Rex domains contain a Rossmann fold — a nucleotide-binding domain capable of binding adenine nucleotides [91–93]. Specificity for a particular nucleotide in Rossmann folds is achieved at specific positions in the polypeptide chain. Rex domains evolved to selectively bind NADH in presence of excess of NAD^+. Peredox and Frex sensors explore changes in the Rex dimerization state upon NADH binding. Incorporating cpFP into an engineered linker between two Rex subunits allowed spectral changes upon NADH binding. Performance of the sensors was tested in cultured mammalian cell lines [26,90]. The cpFP core of Peredox is pH-stable, but intensiometric. To enable ratiometric readout, the entire sensor was fused with red fluorescent protein [26]. Extremely high sensitivity of Peredox to NADH precludes its use in the mitochondrial matrix where NAD^+/NADH ratio is low. The Frex sensor is based on cpYFP and, therefore needs pH control [90].

4. How to use them?

The first question when planning using redox GEFIs should be: what is the substance I want to measure? A number of papers report use of roGFP as a probe for ROS, which is completely wrong. In fact, roGFPs do not react with ROS under physiological conditions because their cysteines have a very low reaction rate with H_2O_2 [68]. They equilibrate with the total thiol pool in the compartment by means of glutaredoxins. The availability of Grx is a rate-limiting factor in the thiol-disulfide exchange between the probe and its environment. It is therefore clear that roGFP2-Grx1 is the probe of choice when measuring thiols redox state [67]. Currently, no superoxide-specific GEFI is available, therefore ROS-detecting sensors are restricted to H_2O_2-detecting HyPer versions [24,50,57] and Orp1-roGFP2 [71].

While both HyPer and roGFP-based probes have been used mostly to reveal spatial and temporal patterns of H_2O_2 production or glutathione redox state, they can be used in a more quantitative way. Both sensors are ratiometric and therefore calibration is possible. Technically, for roGFP2 ratio values should be obtained for completely reduced and completely oxidized probe and then for the experimental condition using exactly the same imaging/fluorimetry settings. Then two equations allow transforming ratio values into E_{GSH}. The description of the procedure and the math behind quantitative roGFP imaging can be found in several papers [67,68,70].

Up to now, HyPer had never been used in quantitative imaging experiments. However, it has been calibrated in vitro against various concentrations of H_2O_2 [24]. Therefore, in principle, HyPer ratio values can be transformed into H_2O_2 values similar to roGFP2 → E_{GSH} transformation. Note, however, that HyPer competes for H_2O_2 with powerful antioxidant systems, like Prx, and the amount of H_2O_2 measured by HyPer can be used as an estimate rather than absolute numbers.

There are several levels of biological system complexity where using redox GEFIs can provide important information. The most obvious application is real time imaging in the living cells. Before the advent of redox GEFIs, dynamic monitoring of redox state was impossible. Intracellular dyes were not specific and extracellular dyes, although specific enough, averaged signals from many cells. GEFIs made it possible to observe processes at the single-cell level for the first time. Given the protein nature of the indicators, the next immediate idea was to target them to the various intracellular compartments: mitochondria, nucleus, cytoplasm, ER and others. But what if measuring H_2O_2 using a probe localized in some compartment gives an average H_2O_2 readout, but the real distribution of the oxidant is more complex, even at the level of the organelle? Fortunately, GEFIs can answer this question. By fusing them to proteins that localize to specific microdomains within the organelle it is possible to track redox processes at the level of the diffraction limit of fluorescent microscopy. An opposite pole of complexity is tissue-scale monitoring of redox events. While technically simple, tissue-scale imaging provides information of great importance.

4.1. HyPer in organelles

HyPer and its derivatives have been successfully used in a number of experimental systems that report H_2O_2 production in response to EGF [94,95], PDGF [57], NGF [24], high frequency electrical stimulation of neurons [96], insulin [97] and other stimuli. In all cases HyPer was used as so-called HyPer-cyto targeted to the nucleocytoplasmic compartment (freely shuttling between the cytoplasm and the nucleus). Most papers report using HyPer in a ratiometric mode, although single-wavelength imaging is possible as well. Since HyPer is composed of protein domains that have no evolved partners in eukaryotic (especially mammalian) cells, it diffuses very rapidly and therefore averages the signal. Indeed, even in the case of local H_2O_2 production the diffusion of the probe makes the actual source obscure. The same can be true for roGFPs as well. As mentioned above, a pH control has to be used in parallel with HyPer. While BCECF-AM was used as a pH control in experiments with NGF [24], most of the above-mentioned physiological stimulation experiments [24,57,94–97] were performed without monitoring pH changes. From our unpublished data obtained with HyPer-C199S we know that EGF and PDGF do not produce measurable changes in cytosolic pH, at least in HeLa and NIH-3T3 cell lines. However, a proper pH control should always be used when possible.

Being targeted to organelles, HyPer has been used to track changes in H_2O_2 in mitochondria [24,51,55,98,99] and peroxisomes [51,53,54]. Although it has not been done yet, coexpression of HyPer located in distinct compartments, such as the nucleus and mitochondria could be used for simultaneous monitoring of the H_2O_2 level in both using confocal microscopy.

4.2. Imaging redox microdomains

Recently, a proteomic study of steady-state Cys oxidation state in different compartments demonstrated that the nucleus, cytoplasm

and mitochondrial matrix did not differ on average in Cys redox state. However, significant differences were found between different pathways in each particular compartment. For example, in cytoplasm, proteins associated with the cytoskeleton demonstrated the highest number of reduced cysteines, whereas the PI3K/Akt pathway had the highest proportion of oxidized residues [100]. It now becomes clear that redox maps of the organelles are highly heterogeneous and include zones of high ROS production and zones where the proteins are kept reduced. Cells have evolved diverse ways to restrict diffusion of potentially harmful ROS within compartments.

HyPer has been used for visualizing the sites of focal ROS production within compartments [52,101]. As diffusion of the probe inside the cell is a major limitation in the imaging of localized H_2O_2, the logical way to improve the spatio-temporal resolution is by immobilizing the sensor inside the cell. Thus, it can be fused with different proteins localized on the cytoplasmic face of the plasma membrane, endosomes and the ER membrane. This has allowed imaging of H_2O_2 microdomain formation upon activation of receptor tyrosine kinases such as EGFR (Fig. 3) and PDGFR. Microdomains of H_2O_2 were found to be associated with activated receptors on endosomes (for EGFR, Fig. 3A,C) and plasma

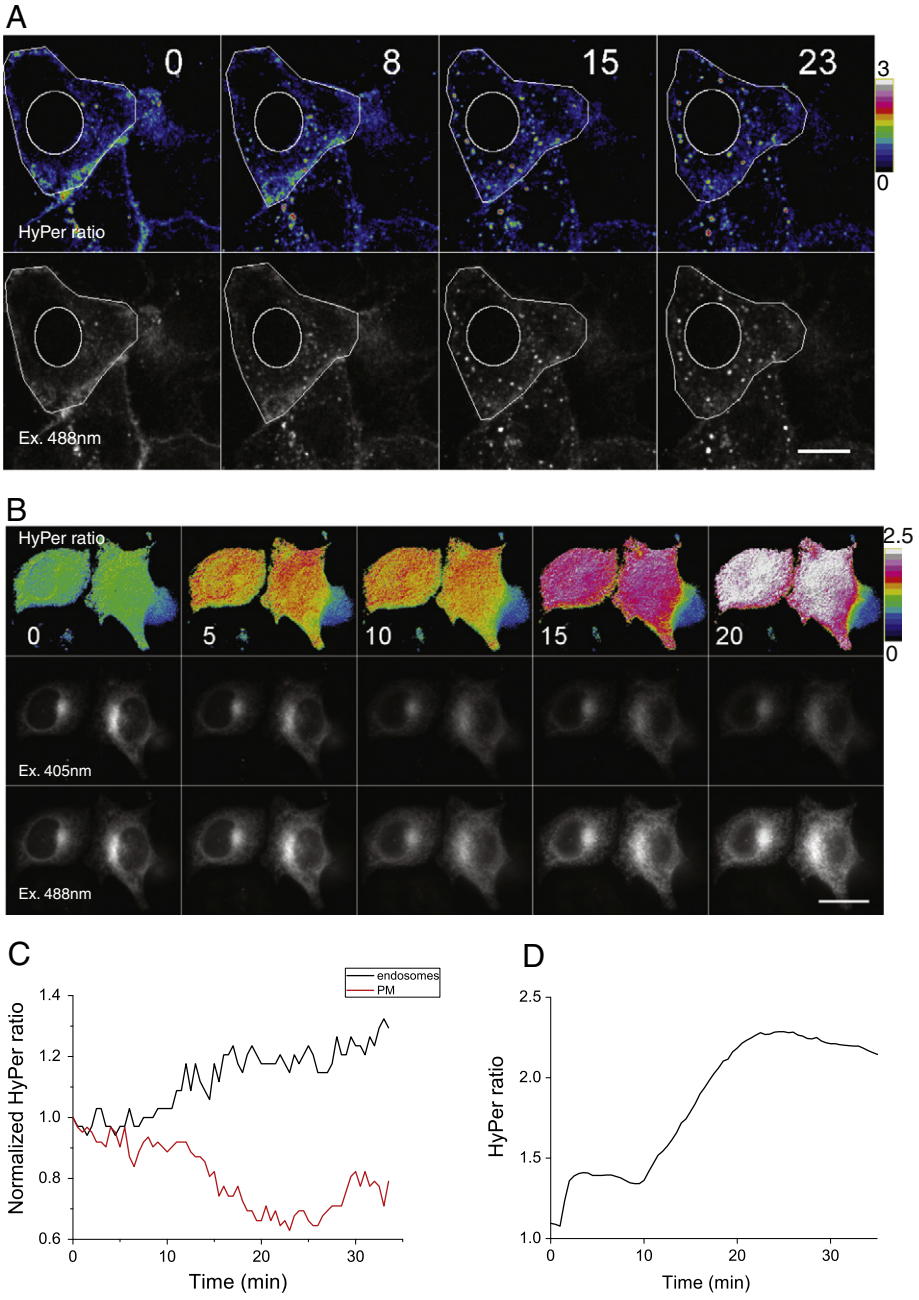

Fig. 3. Microdomains of elevated H_2O_2 generation upon activation of EGFR. A. Confocal images of EGFR-HyPer expressing HeLa-Kyoto cells at indicated time points (in minutes) after stimulation of the cells with 50 ng/ml EGF. Upper row of images represents subcellular distribution of HyPer ratio. Lower row of images shows subcellular distribution of EGFR-HyPer. Cell boundaries and nucleus of one of the cells are highlighted. Scale bar 15 μm. B. Dynamics of H_2O_2 near the cytoplasmic surface of the ER. Widefield fluorescence images of HyPer-TA expressing HeLa-Kyoto cells at indicated time points (in minutes) after stimulation of the cells with 50 ng/ml EGF. Upper row of images represent subcellular distribution of HyPer ratio. Middle and lower rows of images show subcellular distribution of HyPer-TA and changes in fluorescence intensity in each imaging channel. Scale bar 15 μm. C. Time course of H_2O_2 production associated with endosomes and PM in the cells shown on panel A. D. Time course of H_2O_2 production by the cells shown in panel B. Figure modified from Mishina et al. [52].

membrane (for PDGFR) and with PTP-1B phosphatase (Fig. 3B,D). The diffusion of H_2O_2 within the cytoplasm appeared to be restricted to less than a 1 μm radius [52].

More specifically, activation of the cells with EGF resulted in rapid internalization of EGFR-HyPer into endosomes (Fig. 3A). However, some of the receptor-probe fusion remained on the plasma membrane allowing a direct comparison between HyPer ratios on the endosomes and on the PM. H_2O_2 production was endosome-specific: while HyPer on the surface of the endosomes became oxidized, PM-associated probe remained reduced. Moreover, the sensor localized near the cell–cell contacts demonstrated reduction. This observation suggested that the endosomes containing internalized receptor served as the compartment responsible for H_2O_2 generation.

Delivering the probe to a cytoplasmic surface of the ER membrane allowed H_2O_2 monitoring in the close vicinity of the redox-regulated phosphatase PTP-1B. Tail-anchored HyPer (HyPer-TA) detected a two-phase increase of H_2O_2 near the surface of the ER membrane (Fig. 3B) upon EGF addition. The temporal pattern of the HyPer-TA ratio differed from that of EGFR-HyPer. The first wave of H_2O_2 started with less than a minute delay after the stimulus and lasted for 10–15 min before a second wave of H_2O_2 of a much higher amplitude followed (Fig. 3C,D).

These data represent the first direct observation of the H_2O_2 microdomains. Importantly, we observed no diffusion of H_2O_2 between PM, ER and endosomal cytoplasmic surfaces while the probes were sometimes saturated indicating concentrations of H_2O_2 more than 200–300 nM.

Could pH contribute to HyPer signal in the models described? We did not use SypHer in fusions with all the proteins mentioned above. However, our unpublished data indicate that global cytoplasmic pH does not change in HeLa-Kyoto and NIH-3T3 cells upon addition of EGF and PDGF, respectively. Moreover, all the signals we measured appeared to be sensitive to inhibition by Nox inhibitor diphenyleniodonium (DPI) at concentrations as low as 5 μM.

Could the ratio changes we see be due to some perimembrane alkalinization? In principle, Nox activity leads to a local release of the protons near the cytoplasmic surfaces of the membranes. Therefore local acidification would be a more likely scenario.

Further investigations will show whether other redox-related molecules are distributed heterogeneously within cell compartments. Not all, but many GEFIs can be fused to various proteins to enable a more precise mapping of redox changes.

4.3. Imaging H_2O_2 in vivo using HyPer

Hydrogen peroxide forms tissue-scale gradients in response to wounding. Niethammer, Grabher and colleagues demonstrated the existence of this gradient in zebrafish *Danio rerio* upon cutting the tail fins of 3 dpf larvae [102]. The gradient acts to attract neutrophils to the site of wounding and represents the earliest event in the inflammatory response. HyPer expression was achieved by injecting mRNA into the oocyte. Transgenesis is also possible: the H_2O_2 gradient was later visualized using HyPer-3 expressed in the transgenic animal under β-actin promoter [50]. Interestingly, later studies showed that neutrophils arriving at the wound dissipate the H_2O_2 gradient by means of myeloperoxidase, an enzyme of antibacterial defense machinery [103]. At the tissue level myeloperoxidase acted as an H_2O_2-scavenging enzyme, efficiently consuming H_2O_2 in the surrounding tissue. Generation of a line of transgenic fish expressing HyPer specifically in the neutrophils enabled the visualization of cell-scale H_2O_2 gradients in the neutrophils migrating to the wound [103].

Recently, HyPer has been used to study an H_2O_2 gradient formed in tadpoles of *Xenopus laevis* upon tail fin amputation [104]. This gradient was found to be necessary to induce regeneration of the fin via Wnt/β-catenine pathway activation. Notably, various antioxidants and inhibitors of NADPH oxidase blocked regeneration, but HyPer expression did not. This argues against a strong antioxidant capacity of the probe. In contrast, peroxidase activity of HyPer has been shown to have physiological effects in *Arabidopsis thaliana* [105].

4.4. In vivo roGFP2 imaging in Drosophila tissues

roGFP2 in its versions fused to Grx1 and Orp1 was used to study age- and condition-related alterations of GSH/GSSG and H_2O_2 in living larval and fixed adult *Drosophila melanogaster* [106]. The Orp1-roGFP2 and roGFP2-Grx1 targeted to the cytoplasm or mitochondrial matrix were expressed in transgenic animals. While the GSH/GSSG level in cytoplasm appeared to be stable in different tissues and in adult flies of different ages (1 to 14 days), mitochondrial GSH/GSSG was more heterogeneous: more oxidized in Malpighian tubules and fat tissue and more reduced in muscles. Both mitochondrial and cytoplasmic H_2O_2 responses demonstrated a high degree of variability between different tissues and different aged flies. Midgut entherocytes were found to be a major source of aging-associated H_2O_2 production. Interestingly, an increase in lifespan was correlated with higher H_2O_2 in the gut. Another important finding was the absence of an antioxidant effect of N-acetyl-cysteine in vivo. The study showed clearly that differences in $[H_2O_2]$ do not correlate with differences in GSH/GSSG and that the two parameters should be considered and measured, separately.

4.5. HyPer in Caenorhabditis elegans: H_2O_2 changes with aging

A study published by the Jakob group reported that in *C. elegans* the H_2O_2 level is high during the development stages, decreases in the early adult stage and remains low before aging when the second burst takes place [107]. Imaging was performed using HyPer and the results were cross-validated using redox proteomics and the Amplex Red assay. In contrast to the results obtained in *Drosophila*, redox imaging of *C. elegans* revealed a negative correlation between high H_2O_2 levels in tissues and lifespan. Interestingly, the worms showing higher H_2O_2 levels during development had higher levels of the oxidant on aging.

4.6. roGFP2-Grx1 in yeasts: active transport of GSSG from cytoplasm maintains GSH/GSSG reduced

Estimating cytoplasmic GSH/GSSG redox state using whole-cell extracts resulted in an approximately100:1 GSH:GSSG ratio corresponding to a glutathione redox potential of −240 mV. However, quantitative measurement of cytosolic E_{GSH} with rxYFP and roGFP2-Grx1 showed a much more reduced GSH/GSSG state (−320 mV) corresponding to a 50,000:1 GSH:GSSG ratio. Morgan and colleagues showed that under oxidative challenge or glutathione reductase Glr1 deficiency highly reducing glutathione state in yeast cells is maintained by rapid active export of GSSG from the cell by ABC-C transporter Ycf1 [108]. Given that MRP1, a mammalian homolog of Ycf1, had earlier been shown to transport GSSG from the cells under oxidative stress conditions [109,110], this mechanism seems to be conserved in eukaryotic species.

4.7. Combining readouts for multiparameter imaging

HyPer and probably other ratiometric GEFIs can be fused not only with organelle-specific tags or proteins of interest, but also with sensors with distinct readout, namely translocation-based. Fusing HyPer with the PH domain from Bruton's tyrosine kinase, specifically sensitive to phosphatydilinositol (3,4,5)-3P, allowed monitoring of both H_2O_2 and PIP3 in a single cell with a single probe [101]. While translocation-based readout reported PIP3 accumulation, ratiometric readout reported H_2O_2. Both PIP3 and H_2O_2 were shown to be highly polarized in T-cells forming immunological synapses.

4.8. Some limitations to consider

While the pH sensitivity and need for adequate pH control with probes like HyPer and rxYFP have been extensively discussed in this and other papers with highlighting the need for adequate pH control, another important question remains unaddressed. How do the probes affect system they have been used in? The answer is not simple. Potentially, sensors like HyPer and Orp1-roGFP2 can have an antioxidant activity and Grx1-roGFP2 might affect proteins thiol redox state in compartments where endogenous Grx is limited. HyPer has a very high reaction rate with H_2O_2 (10^5 M^{-1} s^{-1}) [50]. The reaction is oxidation-based and leads to the reduction of H_2O_2. Therefore, HyPer can be considered as an antioxidant. However, its antioxidant properties depend on reducing activity of Grx or Trx. While the oxidation of the probe takes seconds, the reduction takes minutes [24,50,57]. Therefore HyPer cannot be considered as an efficient antioxidant. Consistent with this, whereas peroxidase activity of HyPer produces physiological effects in *A. thaliana* [105], in other systems even a strong expression of HyPer does not mimic effects of antioxidants: examples are wound healing [102] and tail fin regeneration [104]. However, more research is needed to understand how local expression of HyPer can alter [H_2O_2] in subcellular compartments. The same is true for Orp1-roGFP2 as the redox kinetics of the probe are similar to HyPer [71].

Overexpression of Grx1-roGFP2 brings extra Grx1 activity to the compartment of interest. This activity can be directed towards not only roGFP2 fused, but also to thiols in other proteins. For example, in yeast mitochondrial intermembrane space where glutaredoxins are limited Grx1-roGFP2 probe shows a more negative E_{GSH} (~300 mV) [111] than rxYFP (−255 mV) [112]. Clearly, this discrepancy is due to the better equilibration of Grx1-roGFP2 with the IMS glutathione pool since there is poor availability of glutaredoxin in the yeast IMS. As roGFP2 and rxYFP are the "model" thiol-containing proteins, the conclusion can be made that elevating the Grx activity in the IMS makes the protein thiol pool there more reduced. Of course, in the case of Grx1-roGFP2 the Grx activity is fused to roGFP2 and therefore the active concentration of Grx in the vicinity of roGFP2 is much higher than can be achieved even upon overexpression. Further experiments with co-expression of roGFP2 with Grx1 both targeted to the IMS could help to clarify this issue. However, it is clear that the possible effects of bringing additional enzymatic activity to cellular compartments have to be carefully considered when using redox probes.

5. Redox-sensitive photoconversions of fluorescent proteins

In 1997, an unusual type of GFP photoconversion (later dubbed "anaerobic redding") was discovered [113,114]. It was found that under low oxygen conditions illumination of GFP results in its conversion into a red fluorescent state with an excitation maximum at 525 nm and a broad emission peak at about 600 nm. This red form is stable for hours in the absence of molecular oxygen, but disappears quickly upon re-oxygenation. Interestingly, green FPs of diverse origin and low sequence similarity undergo anaerobic redding [115]. Today, more than 15 years after its discovery, the molecular mechanism for this photoconversion remains unknown. From indirect evidence, it has been hypothesized that red GFP results from photoreduction and carries the chromophore in a stable radical state [115].

As efficiency of anaerobic GFP redding strongly depends on oxygen level (it should be <2%), it was proposed to use it to indicate local oxygenation level [116]. Using this approach, diffusion gradients of oxygen were measured in cell culture models [117]. Interestingly, even an intracellular O_2 gradient can be detected with photoconversion of a mitochondria-targeted GFP [117]. The photoinduced appearance of a red GFP form was also demonstrated in ischemic liver and kidney in the GFP-transgenic green mouse (for photoconversion and imaging the organs were exposed and covered with a polymeric film to prevent oxygen diffusion from the atmosphere) [118].

Another type of redox-dependent green-to-red GFP photoconversion ("oxidative redding") has been described, recently [119]. In contrast to the above mentioned anaerobic photoconversion, it occurs under normal oxygenated conditions. In oxidative redding, excited GFP donates two electrons to appropriate electron acceptors and becomes red fluorescent with excitation and emission maxima at 585 and 610 nm, respectively. It was found that biologically relevant redox-active molecules, such as flavins, flavoproteins, and cytochromes, can mediate GFP photoconversion. Importantly, oxidative GFP photoconversion can be induced not only in vitro, but also in live cells with no external addition of oxidants. Thus, GFP can meet some intracellular electron acceptors and donate electrons to them. Experiments with cell culture media showed that riboflavin represents the main cause of GFP oxidative redding [120]. At the same time, different efficiencies of this type of photoconversion were observed in different intracellular compartments and in different cell lines [119]. Thus, we believe that oxidative green-to-red photoconversion of GFP can potentially be used as an indicator of some important aspects of intracellular redox environment. Moreover, the ability of GFP to donate electrons can possibly be applied as an optogenetic tool to induce target redox processes. However, further studies on mechanisms of oxidative redding in live cells are required to clarify its practical utility.

The application of both anaerobic and oxidative GFP redding as indicators does have limitations. First, mainly static (endpoint) not dynamic imaging is possible. Second, a strong activating light can damage living cells. Third, the red GFP signal is rather dim and can be clearly detected only at high expression levels of GFP. At the same time, redding is characteristic for commonly used GFPs (e.g., EGFP and AcGFP1), and thus it provides a wide range of ready-to-use transgenic models.

6. Future directions

Redox GEFIs enabled real-time monitoring of H_2O_2, GSH/GSSG and NAD^+/NADH redox state. What are the future directions in redox GEFIs development? Like most of the FP-based sensors, current GEFIs emit light in the green part of the visible spectrum. This means they cannot be used for simultaneous imaging with other green-emitting probes. Therefore, red fluorescent sensors for H_2O_2, GSH/GSSG and other redox couples are in high demand. Recent progress with red GEFIs for Ca^{2+} [28] suggests that red redox probes will soon be available. Improving the properties of the existing probes, such as brightness and photostability, is also a prospective direction.

Whereas red GEFIs have already appeared, far-red sensors have a less clear future. Far-red probes have potential utility because the "optical window" of tissues allows a penetration of light in a near-IR range. Fluorescent protein developers spent more than a decade to obtain the first near far-red FPs [121]. However, most of them have large Stocks shift: they emit in the near-far-red and are excited by an orange light. Therefore, excitation light penetration in tissues can still be a limiting factor. Recently, non-GFP-like far red proteins were designed based on biliverdin-binding bacteriophytochromes [122,123]. While they have very low quantum yield and their performance in fluorescent probes has still to be checked, their spectral properties make them promising fluorescent domains for in vivo deep-in-tissue imaging.

Several reactive oxygen intermediates are still to be visualized. While the utility of cpYFP as a superoxide probe is a matter of debate, other ways to make superoxide sensors are possible. In our opinion, the most promising way is using FeS-cluster containing proteins such as SoxR [45] or aconitase [124–126]. FeS clusters are primary targets of superoxide. Having the reaction rate with superoxide of 10^6–10^7 M^{-1} s^{-1}, FeS clusters can compete for superoxide with SOD. Other molecules that have remained hidden from a direct observation for several decades are nitric oxide and oxygen. Cells evolved protein domains that sense all the factors critical for their existence.

This gives us hope that these domains will be used in future to make the GEFIs for O_2, NO and other important redox-related molecules.

Acknowledgements

We thank Christine Winterbourn and Mike Winterbourn for kindly commenting and editing the text. The work was supported by the Russian Foundation for Basic Research (10-04-01561-a and 11-04-01427-a), a joint EMBL-RFBR grant (12-04-92427), Russian Ministry of Education and Science (11.G34.31.0071) and the Molecular and Cell Biology Program of Russian Academy of Sciences.

References

[1] A.A. Pakhomov, V.I. Martynov, GFP family: structural insights into spectral tuning, Chem. Biol. 15 (2008) 755–764.
[2] F.V. Subach, V.V. Verkhusha, Chromophore transformations in red fluorescent proteins, Chem. Rev. 112 (2012) 4308–4327.
[3] D.M. Chudakov, M.V. Matz, S. Lukyanov, K.A. Lukyanov, Fluorescent proteins and their applications in imaging living cells and tissues, Physiol. Rev. 90 (2010) 1103–1163.
[4] A. Miyawaki, Green fluorescent protein glows gold, Cell 135 (2008) 987–990.
[5] O. Shimomura, F.H. Johnson, Y. Saiga, Extraction, purification and properties of aequorin, a bioluminescent protein from the luminous hydromedusan, *Aequorea*, J. Cell Comp. Physiol. 59 (1962) 223–239.
[6] F.S. Wouters, P.I. Bastiaens, Imaging protein–protein interactions by fluorescence resonance energy transfer (FRET) microscopy, Chapter 5, Curr. Protoc. Neurosci. (2006), (Unit 5 22).
[7] S.B. VanEngelenburg, A.E. Palmer, Fluorescent biosensors of protein function, Curr. Opin. Chem. Biol. 12 (2008) 60–65.
[8] H.J. Carlson, R.E. Campbell, Genetically encoded FRET-based biosensors for multiparameter fluorescence imaging, Curr. Opin. Biotechnol. 20 (2009) 19–27.
[9] G.S. Baird, D.A. Zacharias, R.Y. Tsien, Circular permutation and receptor insertion within green fluorescent proteins, Proc. Natl. Acad. Sci. U.S.A. 96 (1999) 11241–11246.
[10] S. Topell, J. Hennecke, R. Glockshuber, Circularly permuted variants of the green fluorescent protein, FEBS Lett. 457 (1999) 283–289.
[11] M.F. Abad, G. Di Benedetto, P.J. Magalhaes, L. Filippin, T. Pozzan, Mitochondrial pH monitored by a new engineered green fluorescent protein mutant, J. Biol. Chem. 279 (2004) 11521–11529.
[12] M. Kneen, J. Farinas, Y. Li, A.S. Verkman, Green fluorescent protein as a noninvasive intracellular pH indicator, Biophys. J. 74 (1998) 1591–1599.
[13] L.J. Galietta, P.M. Haggie, A.S. Verkman, Green fluorescent protein-based halide indicators with improved chloride and iodide affinities, FEBS Lett. 499 (2001) 220–224.
[14] O. Griesbeck, G.S. Baird, R.E. Campbell, D.A. Zacharias, R.Y. Tsien, Reducing the environmental sensitivity of yellow fluorescent protein, mechanism and applications, J. Biol. Chem. 276 (2001) 29188–29194.
[15] S. Jayaraman, P. Haggie, R.M. Wachter, S.J. Remington, A.S. Verkman, Mechanism and cellular applications of a green fluorescent protein-based halide sensor, J. Biol. Chem. 275 (2000) 6047–6050.
[16] R.M. Wachter, S.J. Remington, Sensitivity of the yellow variant of green fluorescent protein to halides and nitrate, Curr. Biol. 9 (1999) R628–R629.
[17] R.M. Wachter, D. Yarbrough, K. Kallio, S.J. Remington, Crystallographic and energetic analysis of binding of selected anions to the yellow variants of green fluorescent protein, J. Mol. Biol. 301 (2000) 157–171.
[18] H.W. Ai, K.L. Hazelwood, M.W. Davidson, R.E. Campbell, Fluorescent protein FRET pairs for ratiometric imaging of dual biosensors, Nat. Methods 5 (2008) 401–403.
[19] A.W. Nguyen, P.S. Daugherty, Evolutionary optimization of fluorescent proteins for intracellular FRET, Nat. Biotechnol. 23 (2005) 355–360.
[20] E.B. van Munster, T.W. Gadella, Fluorescence lifetime imaging microscopy (FLIM), Adv. Biochem. Eng. Biotechnol. 95 (2005) 143–175.
[21] J. Zhang, R.E. Campbell, A.Y. Ting, R.Y. Tsien, Creating new fluorescent probes for cell biology, Nat. Rev. Mol. Cell Biol. 3 (2002) 906–918.
[22] T. Nagai, A. Sawano, E.S. Park, A. Miyawaki, Circularly permuted green fluorescent proteins engineered to sense Ca^{2+}, Proc. Natl. Acad. Sci. U.S.A. 98 (2001) 3197–3202.
[23] J. Nakai, M. Ohkura, K. Imoto, A high signal-to-noise Ca(2+) probe composed of a single green fluorescent protein, Nat. Biotechnol. 19 (2001) 137–141.
[24] V.V. Belousov, A.F. Fradkov, K.A. Lukyanov, D.B. Staroverov, K.S. Shakhbazov, A.V. Terskikh, S. Lukyanov, Genetically encoded fluorescent indicator for intracellular hydrogen peroxide, Nat. Methods 3 (2006) 281–286.
[25] J. Berg, Y.P. Hung, G. Yellen, A genetically encoded fluorescent reporter of ATP: ADP ratio, Nat. Methods 6 (2009) 161–166.
[26] Y.P. Hung, J.G. Albeck, M. Tantama, G. Yellen, Imaging cytosolic NADH–NAD(+) redox state with a genetically encoded fluorescent biosensor, Cell Metab. 14 (2011) 545–554.
[27] B. Simen Zhao, Y. Liang, Y. Song, C. Zheng, Z. Hao, P.R. Chen, A highly selective fluorescent probe for visualization of organic hydroperoxides in living cells, J. Am. Chem. Soc. 132 (2010) 17065–17067.
[28] Y. Zhao, S. Araki, J. Wu, T. Teramoto, Y.F. Chang, M. Nakano, A.S. Abdelfattah, M. Fujiwara, T. Ishihara, T. Nagai, R.E. Campbell, An expanded palette of genetically encoded Ca(2)(+) indicators, Science 333 (2011) 1888–1891.
[29] C. Schultz, A. Schleifenbaum, J. Goedhart, T.W. Gadella Jr., Multiparameter imaging for the analysis of intracellular signaling, ChemBioChem 6 (2005) 1323–1330.
[30] T. Balla, P. Varnai, Visualization of cellular phosphoinositide pools with GFP-fused protein-domains, Chapter 24, Curr. Protoc. Cell Biol. (2009), (Unit 24. 4).
[31] P. Varnai, T. Balla, Live cell imaging of phosphoinositide dynamics with fluorescent protein domains, Biochim. Biophys. Acta 1761 (2006) 957–967.
[32] G. Halet, Imaging phosphoinositide dynamics using GFP-tagged protein domains, Biol. Cell 97 (2005) 501–518.
[33] G. Nelson, L. Paraoan, D.G. Spiller, G.J. Wilde, M.A. Browne, P.K. Djali, J.F. Unitt, E. Sullivan, E. Floettmann, M.R. White, Multi-parameter analysis of the kinetics of NF-kappaB signalling and transcription in single living cells, J. Cell Sci. 115 (2002) 1137–1148.
[34] J.A. Schmid, A. Birbach, R. Hofer-Warbinek, M. Pengg, U. Burner, P.G. Furtmuller, B.R. Binder, R. de Martin, Dynamics of NF kappa B and Ikappa Balpha studied with green fluorescent protein (GFP) fusion proteins. Investigation of GFP-p65 binding to DNa by fluorescence resonance energy transfer, J. Biol. Chem. 275 (2000) 17035–17042.
[35] L. Zhang, N.G. Gurskaya, E.M. Merzlyak, D.B. Staroverov, N.N. Mudrik, O.N. Samarkina, L.M. Vinokurov, S. Lukyanov, K.A. Lukyanov, Method for real-time monitoring of protein degradation at the single cell level, Biotechniques 42 (446) (2007) 448–450.
[36] J. Chu, Z. Zhang, Y. Zheng, J. Yang, L. Qin, J. Lu, Z.L. Huang, S. Zeng, Q. Luo, A novel far-red bimolecular fluorescence complementation system that allows for efficient visualization of protein interactions under physiological conditions, Biosens. Bioelectron. 25 (2009) 234–239.
[37] S. Cabantous, T.C. Terwilliger, G.S. Waldo, Protein tagging and detection with engineered self-assembling fragments of green fluorescent protein, Nat. Biotechnol. 23 (2005) 102–107.
[38] H. Ostergaard, A. Henriksen, F.G. Hansen, J.R. Winther, Shedding light on disulfide bond formation: engineering a redox switch in green fluorescent protein, EMBO J. 20 (2001) 5853–5862.
[39] G.T. Hanson, R. Aggeler, D. Oglesbee, M. Cannon, R.A. Capaldi, R.Y. Tsien, S.J. Remington, Investigating mitochondrial redox potential with redox-sensitive green fluorescent protein indicators, J. Biol. Chem. 279 (2004) 13044–13053.
[40] C.T. Dooley, T.M. Dore, G.T. Hanson, W.C. Jackson, S.J. Remington, R.Y. Tsien, Imaging dynamic redox changes in mammalian cells with green fluorescent protein indicators, J. Biol. Chem. 279 (2004) 22284–22293.
[41] C. Rota, Y.C. Fann, R.P. Mason, Phenoxyl free radical formation during the oxidation of the fluorescent dye 2′,7′-dichlorofluorescein by horseradish peroxidase. Possible consequences for oxidative stress measurements, J. Biol. Chem. 274 (1999) 28161–28168.
[42] C. Rota, C.F. Chignell, R.P. Mason, Evidence for free radical formation during the oxidation of 2′-7′-dichlorofluorescin to the fluorescent dye 2′-7′-dichlorofluorescein by horseradish peroxidase: possible implications for oxidative stress measurements, Free Radic. Biol. Med. 27 (1999) 873–881.
[43] E. Marchesi, C. Rota, Y.C. Fann, C.F. Chignell, R.P. Mason, Photoreduction of the fluorescent dye 2′-7′-dichlorofluorescein: a spin trapping and direct electron spin resonance study with implications for oxidative stress measurements, Free Radic. Biol. Med. 26 (1999) 148–161.
[44] M.G. Bonini, C. Rota, A. Tomasi, R.P. Mason, The oxidation of 2′,7′-dichlorofluorescin to reactive oxygen species: a self-fulfilling prophesy? Free Radic. Biol. Med. 40 (2006) 968–975.
[45] M. Fujikawa, K. Kobayashi, T. Kozawa, Direct oxidation of the [2Fe-2S] cluster in SoxR protein by superoxide: distinct differential sensitivity to superoxide-mediated signal transduction, J. Biol. Chem. 287 (2012) 35702–35708.
[46] M. Zheng, F. Aslund, G. Storz, Activation of the OxyR transcription factor by reversible disulfide bond formation, Science 279 (1998) 1718–1721.
[47] H. Choi, S. Kim, P. Mukhopadhyay, S. Cho, J. Woo, G. Storz, S. Ryu, Structural basis of the redox switch in the OxyR transcription factor, Cell 105 (2001) 103–113.
[48] F. Aslund, M. Zheng, J. Beckwith, G. Storz, Regulation of the OxyR transcription factor by hydrogen peroxide and the cellular thiol-disulfide status, Proc. Natl. Acad. Sci. U.S.A. 96 (1999) 6161–6165.
[49] C. Lee, S.M. Lee, P. Mukhopadhyay, S.J. Kim, S.C. Lee, W.S. Ahn, M.H. Yu, G. Storz, S.E. Ryu, Redox regulation of OxyR requires specific disulfide bond formation involving a rapid kinetic reaction path, Nat. Struct. Mol. Biol. 11 (2004) 1179–1185.
[50] D.S. Bilan, L. Pase, L. Joosen, A.Y. Gorokhovatsky, Y.G. Ermakova, T.W. Gadella, C. Grabher, C. Schultz, S. Lukyanov, V.V. Belousov, HyPer-3: a genetically encoded H_2O_2 probe with improved performance for ratiometric and fluorescence lifetime imaging, ACS Chem. Biol. 8 (2013) 535–542.
[51] M. Malinouski, Y. Zhou, V.V. Belousov, D.L. Hatfield, V.N. Gladyshev, Hydrogen peroxide probes directed to different cellular compartments, PLoS One 6 (2011) e14564.
[52] N.M. Mishina, P.A. Tyurin-Kuzmin, K.N. Markvicheva, A.V. Vorotnikov, V.A. Tkachuk, V. Laketa, C. Schultz, S. Lukyanov, V.V. Belousov, Does cellular hydrogen peroxide diffuse or act locally? Antioxid. Redox Signal. 14 (2011) 1–7.
[53] A. Costa, I. Drago, S. Behera, M. Zottini, P. Pizzo, J.I. Schroeder, T. Pozzan, F. Lo Schiavo, H_2O_2 in plant peroxisomes: an in vivo analysis uncovers a Ca(2+)-dependent scavenging system, Plant J. 62 (2010) 760–772.
[54] M. Elsner, W. Gehrmann, S. Lenzen, Peroxisome-generated hydrogen peroxide as important mediator of lipotoxicity in insulin-producing cells, Diabetes 60 (2011) 200–208.
[55] R.F. Wu, Z. Ma, Z. Liu, L.S. Terada, Nox4-derived H_2O_2 mediates endoplasmic reticulum signaling through local Ras activation, Mol. Cell. Biol. 30 (2010) 3553–3568.

[56] B. Enyedi, P. Varnai, M. Geiszt, Redox state of the endoplasmic reticulum is controlled by Ero1L-alpha and intraluminal calcium, Antioxid. Redox Signal. 13 (2010) 721–729.
[57] K.N. Markvicheva, D.S. Bilan, N.M. Mishina, A.Y. Gorokhovatsky, L.M. Vinokurov, S. Lukyanov, V.V. Belousov, A genetically encoded sensor for H_2O_2 with expanded dynamic range, Bioorg. Med. Chem. 19 (2011) 1079–1084.
[58] K. Brejc, T.K. Sixma, P.A. Kitts, S.R. Kain, R.Y. Tsien, M. Ormo, S.J. Remington, Structural basis for dual excitation and photoisomerization of the Aequorea victoria green fluorescent protein, Proc. Natl. Acad. Sci. U.S.A. 94 (1997) 2306–2311.
[59] M.A. Elsliger, R.M. Wachter, G.T. Hanson, K. Kallio, S.J. Remington, Structural and spectral response of green fluorescent protein variants to changes in pH, Biochemistry 38 (1999) 5296–5301.
[60] G.T. Hanson, T.B. McAnaney, E.S. Park, M.E. Rendell, D.K. Yarbrough, S. Chu, L. Xi, S.G. Boxer, M.H. Montrose, S.J. Remington, Green fluorescent protein variants as ratiometric dual emission pH sensors. 1. Structural characterization and preliminary application, Biochemistry 41 (2002) 15477–15488.
[61] D. Poburko, J. Santo-Domingo, N. Demaurex, Dynamic regulation of the mitochondrial proton gradient during cytosolic calcium elevations, J. Biol. Chem. 286 (2011) 11672–11684.
[62] M. Tantama, Y.P. Hung, G. Yellen, Imaging intracellular pH in live cells with a genetically encoded red fluorescent protein sensor, J. Am. Chem. Soc. 133 (2011) 10034–10037.
[63] Y. Li, R.W. Tsien, pHTomato, a red, genetically encoded indicator that enables multiplex interrogation of synaptic activity, Nat. Neurosci. 15 (2012) 1047–1053.
[64] G. Maulucci, V. Labate, M. Mele, E. Panieri, G. Arcovito, T. Galeotti, H. Ostergaard, J.R. Winther, M. De Spirito, G. Pani, High-resolution imaging of redox signaling in live cells through an oxidation-sensitive yellow fluorescent protein, Sci. Signal. 1 (2008) pl3.
[65] H. Ostergaard, C. Tachibana, J.R. Winther, Monitoring disulfide bond formation in the eukaryotic cytosol, J. Cell Biol. 166 (2004) 337–345.
[66] O. Bjornberg, H. Ostergaard, J.R. Winther, Mechanistic insight provided by glutaredoxin within a fusion to redox-sensitive yellow fluorescent protein, Biochemistry 45 (2006) 2362–2371.
[67] M. Gutscher, A.L. Pauleau, L. Marty, T. Brach, G.H. Wabnitz, Y. Samstag, A.J. Meyer, T.P. Dick, Real-time imaging of the intracellular glutathione redox potential, Nat. Methods 5 (2008) 553–559.
[68] A.J. Meyer, T.P. Dick, Fluorescent protein-based redox probes, Antioxid. Redox Signal. 13 (2010) 621–650.
[69] A.J. Meyer, T. Brach, L. Marty, S. Kreye, N. Rouhier, J.P. Jacquot, R. Hell, Redox-sensitive GFP in Arabidopsis thaliana is a quantitative biosensor for the redox potential of the cellular glutathione redox buffer, Plant J. 52 (2007) 973–986.
[70] B. Morgan, M.C. Sobotta, T.P. Dick, Measuring E(GSH) and H_2O_2 with roGFP2-based redox probes, Free Radic. Biol. Med. 51 (2012) 1943–1951.
[71] M. Gutscher, M.C. Sobotta, G.H. Wabnitz, S. Ballikaya, A.J. Meyer, Y. Samstag, T.P. Dick, Proximity-based protein thiol oxidation by H_2O_2-scavenging peroxidases, J. Biol. Chem. 284 (2009) 31532–31540.
[72] S.R. Lee, K.S. Kwon, S.R. Kim, S.G. Rhee, Reversible inactivation of protein-tyrosine phosphatase 1B in A431 cells stimulated with epidermal growth factor, J. Biol. Chem. 273 (1998) 15366–15372.
[73] Y.W. Lou, Y.Y. Chen, S.F. Hsu, R.K. Chen, C.L. Lee, K.H. Khoo, N.K. Tonks, T.C. Meng, Redox regulation of the protein tyrosine phosphatase PTP1B in cancer cells, FEBS J. 275 (2008) 69–88.
[74] C.C. Winterbourn, Reconciling the chemistry and biology of reactive oxygen species, Nat. Chem. Biol. 4 (2008) 278–286.
[75] A. Delaunay, D. Pflieger, M.B. Barrault, J. Vinh, M.B. Toledano, A thiol peroxidase is an H_2O_2 receptor and redox-transducer in gene activation, Cell 111 (2002) 471–481.
[76] V.L. Kolossov, B.Q. Spring, A. Sokolowski, J.E. Conour, R.M. Clegg, P.J. Kenis, H.R. Gaskins, Engineering redox-sensitive linkers for genetically encoded FRET-based biosensors, Exp. Biol. Med. (Maywood) 233 (2008) 238–248.
[77] V.L. Kolossov, B.Q. Spring, R.M. Clegg, J.J. Henry, A. Sokolowski, P.J. Kenis, H.R. Gaskins, Development of a high-dynamic range, GFP-based FRET probe sensitive to oxidative microenvironments, Exp. Biol. Med. (Maywood) 236 (2011) 681–691.
[78] V.L. Kolossov, M.T. Leslie, A. Chatterjee, B.M. Sheehan, P.J. Kenis, H.R. Gaskins, Forster resonance energy transfer-based sensor targeting endoplasmic reticulum reveals highly oxidative environment, Exp. Biol. Med. (Maywood) 237 (2012) 652–662.
[79] J.R. Lohman, S.J. Remington, Development of a family of redox-sensitive green fluorescent protein indicators for use in relatively oxidizing subcellular environments, Biochemistry 47 (2008) 8678–8688.
[80] B. Enyedi, M. Zana, A. Donko, M. Geiszt, Spatial and temporal analysis of NADPH oxidase-generated hydrogen peroxide signals by novel fluorescent reporter proteins, Antioxid. Redox Signal. (2012), http://dx.doi.org/10.1089/ars.2012.4594.
[81] W. Wang, H. Fang, L. Groom, A. Cheng, W. Zhang, J. Liu, X. Wang, K. Li, P. Han, M. Zheng, J. Yin, M.P. Mattson, J.P. Kao, E.G. Lakatta, S.S. Sheu, K. Ouyang, J. Chen, R.T. Dirksen, H. Cheng, Superoxide flashes in single mitochondria, Cell 134 (2008) 279–290.
[82] F.L. Muller, A critical evaluation of cpYFP as a probe for superoxide, Free Radic. Biol. Med. 47 (2009) 1779–1780.
[83] M. Schwarzlander, D.C. Logan, M.D. Fricker, L.J. Sweetlove, The circularly permuted yellow fluorescent protein cpYFP that has been used as a superoxide probe is highly responsive to pH but not superoxide in mitochondria: implications for the existence of superoxide 'flashes', Biochem. J. 437 (2011) 381–387.
[84] M. Schwarzlander, M.P. Murphy, M.R. Duchen, D.C. Logan, M.D. Fricker, A.P. Halestrap, F.L. Muller, R. Rizzuto, T.P. Dick, A.J. Meyer, L.J. Sweetlove, Mitochondrial 'flashes': a radical concept repHined, Trends Cell Biol. 22 (2012) 503–508.
[85] E. Quatresous, C. Legrand, S. Pouvreau, Mitochondria-targeted cpYFP: pH or superoxide sensor? J. Gen. Physiol. 140 (2012) 567–570.
[86] N. Pollak, C. Dolle, M. Ziegler, The power to reduce: pyridine nucleotides — small molecules with a multitude of functions, Biochem. J. 402 (2007) 205–218.
[87] A.A. Starkov, The role of mitochondria in reactive oxygen species metabolism and signaling, Ann. N. Y. Acad. Sci. 1147 (2008) 37–52.
[88] K. Bedard, K.H. Krause, The NOX family of ROS-generating NADPH oxidases: physiology and pathophysiology, Physiol. Rev. 87 (2007) 245–313.
[89] A. Holmgren, C. Johansson, C. Berndt, M.E. Lonn, C. Hudemann, C.H. Lillig, Thiol redox control via thioredoxin and glutaredoxin systems, Biochem. Soc. Trans. 33 (2005) 1375–1377.
[90] Y. Zhao, J. Jin, Q. Hu, H.M. Zhou, J. Yi, Z. Yu, L. Xu, X. Wang, Y. Yang, J. Loscalzo, Genetically encoded fluorescent sensors for intracellular NADH detection, Cell Metab. 14 (2012) 555–566.
[91] K.J. McLaughlin, C.M. Strain-Damerell, K. Xie, D. Brekasis, A.S. Soares, M.S. Paget, C.L. Kielkopf, Structural basis for NADH/NAD + redox sensing by a Rex family repressor, Mol. Cell 38 (2010) 563–575.
[92] E.A. Sickmier, D. Brekasis, S. Paranawithana, J.B. Bonanno, M.S. Paget, S.K. Burley, C.L. Kielkopf, X-ray structure of a Rex-family repressor/NADH complex insights into the mechanism of redox sensing, Structure 13 (2005) 43–54.
[93] E. Wang, M.C. Bauer, A. Rogstam, S. Linse, D.T. Logan, C. von Wachenfeldt, Structure and functional properties of the *Bacillus subtilis* transcriptional repressor Rex, Mol. Microbiol. 69 (2008) 466–478.
[94] K.N. Markvicheva, E.A. Bogdanova, D.B. Staroverov, S. Lukyanov, V.V. Belousov, Imaging of intracellular hydrogen peroxide production with HyPer upon stimulation of HeLa cells with epidermal growth factor, Methods Mol. Biol. 476 (2008) 79–86.
[95] E.W. Miller, B.C. Dickinson, C.J. Chang, Aquaporin-3 mediates hydrogen peroxide uptake to regulate downstream intracellular signaling, Proc. Natl. Acad. Sci. U.S.A. 107 (2010) 15681–15686.
[96] D. Riquelme, A. Alvarez, N. Leal, T. Adasme, I. Espinoza, J.A. Valdes, N. Troncoso, S. Hartel, J. Hidalgo, C. Hidalgo, M.A. Carrasco, High-frequency field stimulation of primary neurons enhances ryanodine receptor-mediated Ca^{2+} release and generates hydrogen peroxide, which jointly stimulate NF-kappaB activity, Antioxid. Redox Signal. 14 (2011) 1245–1259.
[97] A. Espinosa, A. Garcia, S. Hartel, C. Hidalgo, E. Jaimovich, NADPH oxidase and hydrogen peroxide mediate insulin-induced calcium increase in skeletal muscle cells, J. Biol. Chem. 284 (2009) 2568–2575.
[98] J. Jiang, A. Maeda, J. Ji, C.J. Baty, S.C. Watkins, J.S. Greenberger, V.E. Kagan, Are mitochondrial reactive oxygen species required for autophagy? Biochem. Biophys. Res. Commun. 412 (2011) 55–60.
[99] Z. Ungvari, N. Labinskyy, P. Mukhopadhyay, J.T. Pinto, Z. Bagi, P. Ballabh, C. Zhang, P. Pacher, A. Csiszar, Resveratrol attenuates mitochondrial oxidative stress in coronary arterial endothelial cells, Am. J. Physiol. Heart Circ. Physiol. 297 (2009) H1876–H1881.
[100] Y.M. Go, D.M. Duong, J. Peng, D.P. Jones, Protein cysteines map to functional networks according to steady-state level of oxidation, J. Proteomics Bioinform. 4 (2012) 196–209.
[101] N.M. Mishina, I. Bogeski, D.A. Bolotin, M. Hoth, B.A. Niemeyer, C. Schultz, E.V. Zagaynova, S. Lukyanov, V.V. Belousov, Can we see PIP(3) and hydrogen peroxide with a single probe? Antioxid. Redox Signal. 17 (3) (2012) 505–512.
[102] P. Niethammer, C. Grabher, A.T. Look, T.J. Mitchison, A tissue-scale gradient of hydrogen peroxide mediates rapid wound detection in zebrafish, Nature 459 (2009) 996–999.
[103] L. Pase, J.E. Layton, C. Wittmann, F. Ellett, C.J. Nowell, C.C. Reyes-Aldasoro, S. Varma, K.L. Rogers, C.J. Hall, M.C. Keightley, P.S. Crosier, C. Grabher, J.K. Heath, S.A. Renshaw, G.J. Lieschke, Neutrophil-delivered myeloperoxidase dampens the hydrogen peroxide burst after tissue wounding in zebrafish, Curr. Biol. 22 (2012) 1818–1824.
[104] N.R. Love, Y. Chen, S. Ishibashi, P. Kritsiligkou, R. Lea, Y. Koh, J.L. Gallop, K. Dorey, E. Amaya, Amputation-induced reactive oxygen species are required for successful *Xenopus* tadpole tail regeneration, Nat. Cell Biol. 15 (2013) 222–228.
[105] S. Bieker, L. Riester, M. Stahl, J. Franzaring, U. Zentgraf, Senescence-specific alteration of hydrogen peroxide levels in *Arabidopsis thaliana* and oilseed rape spring variety *Brassica napus* L. cv. Mozart, J. Integr. Plant Biol. 54 (2012) 540–554.
[106] S.C. Albrecht, A.G. Barata, J. Grosshans, A.A. Teleman, T.P. Dick, In vivo mapping of hydrogen peroxide and oxidized glutathione reveals chemical and regional specificity of redox homeostasis, Cell Metab. 14 (2012) 819–829.
[107] D. Knoefler, M. Thamsen, M. Koniczek, N.J. Niemuth, A.K. Diederich, U. Jakob, Quantitative in vivo redox sensors uncover oxidative stress as an early event in life, Mol. Cell 47 (2012) 767–776.
[108] B. Morgan, D. Ezerina, T.N. Amoako, J. Riemer, M. Seedorf, T.P. Dick, Multiple glutathione disulfide removal pathways mediate cytosolic redox homeostasis, Nat. Chem. Biol. 9 (2013) 119–125.
[109] J. Hirrlinger, J. Konig, D. Keppler, J. Lindenau, J.B. Schulz, R. Dringen, The multidrug resistance protein MRP1 mediates the release of glutathione disulfide from rat astrocytes during oxidative stress, J. Neurochem. 76 (2001) 627–636.
[110] T. Minich, J. Riemer, J.B. Schulz, P. Wielinga, J. Wijnholds, R. Dringen, The multidrug resistance protein 1 (Mrp1), but not Mrp5, mediates export of glutathione and glutathione disulfide from brain astrocytes, J. Neurochem. 97 (2006) 373–384.
[111] K. Kojer, M. Bien, H. Gangel, B. Morgan, T.P. Dick, J. Riemer, Glutathione redox potential in the mitochondrial intermembrane space is linked to the cytosol and impacts the Mia40 redox state, EMBO J. 31 (2012) 3169–3182.
[112] J. Hu, L. Dong, C.E. Outten, The redox environment in the mitochondrial intermembrane space is maintained separately from the cytosol and matrix, J. Biol. Chem. 283 (2008) 29126–29134.

[113] M.B. Elowitz, M.G. Surette, P.E. Wolf, J. Stock, S. Leibler, Photoactivation turns green fluorescent protein red, Curr. Biol. 7 (1997) 809–812.
[114] K.E. Sawin, P. Nurse, Photoactivation of green fluorescent protein, Curr. Biol. 7 (1997) R606–R607.
[115] V. Kiseleva Iu, A.S. Mishin, A.M. Bogdanov, A. Labas Iu, K.A. Luk'ianov, The ability of green fluorescent proteins for photoconversion under oxygen-free conditions is determined by the chromophore structure rather than its amino acid environment, Bioorg. Khim. 34 (2008) 711–715.
[116] E. Takahashi, T. Takano, A. Numata, N. Hayashi, S. Okano, O. Nakajima, Y. Nomura, M. Sato, Genetic oxygen sensor: GFP as an indicator of intracellular oxygenation, Adv. Exp. Med. Biol. 566 (2005) 39–44.
[117] E. Takahashi, M. Sato, Imaging of oxygen gradients in monolayer cultured cells using green fluorescent protein, Am. J. Physiol. Cell Physiol. 299 (2010) C1318–C1323.
[118] E. Takahashi, T. Takano, Y. Nomura, S. Okano, O. Nakajima, M. Sato, In vivo oxygen imaging using green fluorescent protein, Am. J. Physiol. Cell Physiol. 291 (2006) C781–C787.
[119] A.M. Bogdanov, A.S. Mishin, I.V. Yampolsky, V.V. Belousov, D.M. Chudakov, F.V. Subach, V.V. Verkhusha, S. Lukyanov, K.A. Lukyanov, Green fluorescent proteins are light-induced electron donors, Nat. Chem. Biol. 5 (2009) 459–461.
[120] A.M. Bogdanov, E.A. Bogdanova, D.M. Chudakov, T.V. Gorodnicheva, S. Lukyanov, K.A. Lukyanov, Cell culture medium affects GFP photostability: a solution, Nat. Methods 6 (2009) 859–860.
[121] D. Shcherbo, E.M. Merzlyak, T.V. Chepurnykh, A.F. Fradkov, G.V. Ermakova, E.A. Solovieva, K.A. Lukyanov, E.A. Bogdanova, A.G. Zaraisky, S. Lukyanov, D.M. Chudakov, Bright far-red fluorescent protein for whole-body imaging, Nat. Methods 4 (2007) 741–746.
[122] G.S. Filonov, K.D. Piatkevich, L.M. Ting, J. Zhang, K. Kim, V.V. Verkhusha, Bright and stable near-infrared fluorescent protein for in vivo imaging, Nat. Biotechnol. 29 (2011) 757–761.
[123] X. Shu, A. Royant, M.Z. Lin, T.A. Aguilera, V. Lev-Ram, P.A. Steinbach, R.Y. Tsien, Mammalian expression of infrared fluorescent proteins engineered from a bacterial phytochrome, Science 324 (2009) 804–807.
[124] P.R. Gardner, Superoxide-driven aconitase FE-S center cycling, Biosci. Rep. 17 (1997) 33–42.
[125] P.R. Gardner, I. Raineri, L.B. Epstein, C.W. White, Superoxide radical and iron modulate aconitase activity in mammalian cells, J. Biol. Chem. 270 (1995) 13399–13405.
[126] P.R. Gardner, I. Fridovich, Inactivation–reactivation of aconitase in *Escherichia coli*, a sensitive measure of superoxide radical, J. Biol. Chem. 267 (1992) 8757–8763.